REPORT DOCUMENTATION PAGE

Form Approved OMB NO. 0704-0188

1. REPORT DATE (DD-MM-YYYY)	2. REPORT TYPE	3. DATES COVERED (From - To)
13-01-2015	Conference Proceeding	-

4. TITLE AND SUBTITLE

A Comparison of Shadowgraphy and X-ray Computed Tomography in Liquid Spray Analysis

5a. CONTRACT NUMBER
W911NF-13-2-0048

5b. GRANT NUMBER

5c. PROGRAM ELEMENT NUMBER
611102

6. AUTHORS

Zachary Lee, Daniel Eichner, Jonathan Tennis, Matthew Ryan, Tyler Sowell, Michael Benson, Bret Van Poppel, Thomas Nelson, Pablo Vasquez Guzman, Rebecca Fahrig, John Eaton, Waldo Hinshaw, Matthew Kurman, Chel Ram Kuson

5d. PROJECT NUMBER

5e. TASK NUMBER

5f. WORK UNIT NUMBER

7. PERFORMING ORGANIZATION NAMES AND ADDRESSES

Stanford University
3160 Porter Drive, Suite 100

Palo Alto, CA 94304 -8445

8. PERFORMING ORGANIZATION REPORT NUMBER

9. SPONSORING/MONITORING AGENCY NAME(S) AND ADDRESS (ES)

U.S. Army Research Office
P.O. Box 12211
Research Triangle Park, NC 27709-2211

10. SPONSOR/MONITOR'S ACRONYM(S)
ARO

11. SPONSOR/MONITOR'S REPORT NUMBER(S)
64070-EG.2

12. DISTRIBUTION AVAILIBILITY STATEMENT

Approved for public release; distribution is unlimited.

13. SUPPLEMENTARY NOTES

The views, opinions and/or findings contained in this report are those of the author(s) and should not contrued as an official Department of the Army position, policy or decision, unless so designated by other documentation.

14. ABSTRACT

This work examines and compares two proven techniques for assessing key characteristics of liquid sprays for combustion applications: shadowgraphy and time-averaged X-ray computed tomography (CT). Atomization has key applications in combustion as it can improve fuel efficiency, increase heat release, and decrease pollutant emissions. To improve the design of fuel injection nozzles, the ability to conduct accurate analyses of sprays is crucial. Key characteristics of the liquid spray, such as mean particle diameter, spray-cone angle, mass distribution, and penetration length give insight into the effectiveness of a nozzle. Shadowgraphy is a relatively inexpensive

15. SUBJECT TERMS

X-ray CT, Spray, Shadowgraphy

16. SECURITY CLASSIFICATION OF:			17. LIMITATION OF ABSTRACT	15. NUMBER OF PAGES	19a. NAME OF RESPONSIBLE PERSON
a. REPORT	b. ABSTRACT	c. THIS PAGE			Rebecca Fahrig
UU	UU	UU	UU		19b. TELEPHONE NUMBER 650-724-3559

Report Title

A Comparison of Shadowgraphy and X-ray Computed Tomography in Liquid Spray Analysis

ABSTRACT

This work examines and compares two proven techniques for assessing key characteristics of liquid sprays for combustion applications: shadowgraphy and time-averaged X-ray computed tomography (CT). Atomization has key applications in combustion as it can improve fuel efficiency, increase heat release, and decrease pollutant emissions. To improve the design of fuel injection nozzles, the ability to conduct accurate analyses of sprays is crucial. Key characteristics of the liquid spray, such as mean particle diameter, spray-cone angle, mass distribution, and penetration length give insight into the effectiveness of a nozzle. Shadowgraphy is a relatively inexpensive method that produces a two-dimensional, instantaneous image of the spray particles or spray called a shadowgram. Shadowgrams can be used for analyzing mean particle size, spray-cone angle, and location of breakup regions. X-ray CT measures the time-averaged X-ray absorption of two-dimensional projection images of spray to produce a three-dimensional reconstruction of the spray. X-ray CT can provide valuable insight into the symmetry and mass distribution of a spray; however, X-ray absorption diminishes rapidly with increased distance from nozzles, thereby limiting analysis to the regions near the nozzle. A detailed comparison of the overall effectiveness and unique insights yielded by the two methods illustrates the unique uses, benefits, and shortcomings of each method. The results confirm that X-ray CT scanning proves more effective in the dense, near-nozzle spray region. Shadowgraphy effectively complements the X-ray CT analysis through particle analysis. It additionally allows for relatively simple spray cone analysis, though it cannot provide quantitative mass distribution analysis.

Conference Name: International Mechanical Engineering Congress and Exposition

Conference Date: November 14, 2014

Proceedings of the ASME 2014 International Mechanical Engineering Congress and Exposition
IMECE2014
November 14-20, 2014, Montreal, Quebec Canada

IMECE2014-38770

A COMPARISON OF SHADOWGRAPHY AND X-RAY COMPUTED TOMOGRAPHY IN LIQUID SPRAY ANALYSIS

Zachary Lee, Daniel Eichner, Jonathan Tennis, Matthew Ryan, Tyler Sowell, Michael Benson, Bret Van Poppel, Thomas Nelson
United States Military Academy
West Point, New York, USA

Pablo Vasquez Guzman, Rebecca Fahrig, John Eaton
Stanford University
Stanford, California, USA

Matthew S. Kurman, Chol-Bum M. Kweon
U.S. Army Research Laboratory
Aberdeen Proving Ground, Maryland, USA

ABSTRACT

This work examines and compares two proven techniques for assessing key characteristics of liquid sprays for combustion applications: shadowgraphy and time-averaged X-ray computed tomography (CT). Atomization has key applications in combustion as it can improve fuel efficiency, increase heat release, and decrease pollutant emissions. To improve the design of fuel injection nozzles, the ability to conduct accurate analyses of sprays is crucial. Key characteristics of the liquid spray, such as mean particle diameter, spray-cone angle, mass distribution, and penetration length give insight into the effectiveness of a nozzle. Shadowgraphy is a relatively inexpensive method that produces a two-dimensional, instantaneous image of the spray particles or spray called a shadowgram. Shadowgrams can be used for analyzing mean particle size, spray-cone angle, and location of breakup regions. X-ray CT measures the time-averaged X-ray absorption of two-dimensional projection images of spray to produce a three-dimensional reconstruction of the spray. X-ray CT can provide valuable insight into the symmetry and mass distribution of a spray; however, X-ray absorption diminishes rapidly with increased distance from nozzles, thereby limiting analysis to the regions near the nozzle. A detailed comparison of the overall effectiveness and insights yielded by the two methods illustrates the unique uses, benefits, and shortcomings of each method. The results confirm that X-ray CT scanning proves more effective in the dense, near-nozzle spray region. Shadowgraphy effectively complements the X-ray CT analysis through particle analysis. It also allows for relatively simple spray cone analysis, though it cannot provide quantitative mass distribution analysis.

INTRODUCTION

A varied and growing array of technologies employs spray nozzles in their processes. Non-intrusive measurement techniques have proved essential in determining the effectiveness of various spray techniques. Understanding the multi-phase flows that occur within atomizers and downstream of the nozzle exit gives insight into optimizing atomizers, particularly for combustion applications. The performance of gas turbine engines and internal combustion engines can be enhanced by improved atomization during combustion because of higher fuel-air mixing, higher efficiency, and less harmful pollutant emissions [1]. Industrial applications of atomization control include agricultural spraying, spray drying, spray painting, and cooling [1-4]. Furthermore, accurate experimentation is necessary to evaluate the quantitative accuracy of computational models, which can predict qualitative spray characteristics [2, 5].

This work examines liquid spray fields measured by shadowgraphy and X-ray computed tomography (CT) on the same two custom-made nozzles. The objective is to examine the effectiveness of combining shadowgraphy and X-ray CT to provide a practical, complete, and robust diagnostic approach for assessing liquid sprays.

BACKGROUND

Many different methods have been used to analyze particular aspects of sprays, though each has limitations. Early work on spray characterization used probe techniques which could affect the spray development [6]. Non-intrusive measurement techniques such as schlieren imaging have been used to visualize the overall spray development. However, schlieren did not produce quantitative information on the spray formation or droplet characteristics, so other optical techniques for quantitative spray measurements were developed. Coghe and Cossali identified several non-intrusive "classic techniques" for investigating spray parameters: Laser Doppler Velocimetry, Phase Doppler Anemometry, Particle Image Velocimetry, Fraunhofer Diffraction, and Quantitative Laser Sheet Visualization [2]. These classic techniques use Mie scattering and Rayleigh scattering to determine the location, size distribution, and velocity of spray droplets.

The optical methods used in this work are shadowgraphy and X-ray computed tomography. In shadowgraphy, a substance refracts light, and the shadow is then recorded. Shadowgraphy can be seen in everyday life from the shadows caused by hot gases from a flame. The shadow is created from light that is refracted when passing through the hot gases, which have a different density, and therefore refractive index, than the surrounding air [7]. Following Robert Hooke's and Jean Paul Marat's initial explorations into shadowgraphy, Victor Dvorak published the first recognized account of shadowgraphy techniques. Dvorak began by investigating mixing in water with a 1-mm aperture and shadows displayed on a white wall [8]. In spray visualization, shadowgraphy involves a light source behind the spray. The light source is in line with a camera, and the shadow of the spray is recorded. Figure 1 illustrates this process, and the experimental setup is shown in Figure 3.

The advantages of shadowgraphy include a relatively simple setup, potential for high-speed acquisition of images, and thin focal regions. This allows for non-intrusive investigation into spray parameters such as droplet size, droplet velocity and spray cone angle. With an ability to take near-instantaneous images (40,000 frames per second in this experiment), shadowgraphy can provide clear images of droplets and their motion in a spray. The technique can also provide basic analysis of the dense near-nozzle region such as spray cone angle and skew, but it cannot distinguish one part of a dense spray from another [6].

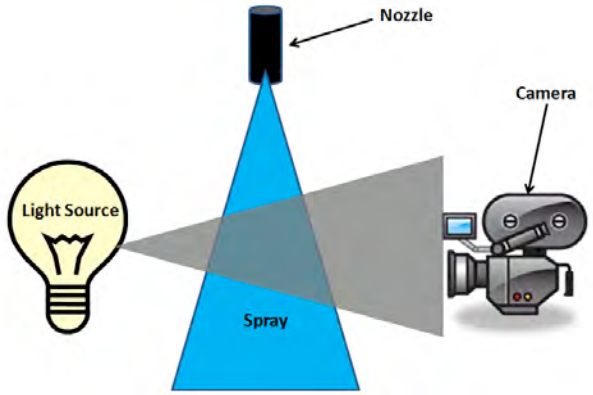

Figure 1: Basic overview of shadowgraphy

The most significant drawback to shadowgraphy is its inability to resolve features of the dense fluid regions near the spray nozzle [9, 10]. Because light refraction by liquid sheets is significant, these areas all cast a full shadow on the camera. As a result, the dense fluid region appears as a singular shadow, which significantly limits detailed data collection in the near nozzle region, defined by Linne to be generally within 0-6 mm, but this can vary with nozzle geometry [6]. Another limitation is the two-dimensional nature of shadowgrams. Due to this property, different orientations can result in slightly different results for nozzle symmetry or shape. Shadowgraphy can only help determine asymmetries in the plane normal to the camera's line of sight for single orientations, though 3D reconstruction is possible with multiple views on a spray [11].

X-ray computed tomography involves combining several two-dimensional X-ray projections into a three-dimensional reconstruction, and it can help overcome many shortcomings associated with shadowgraphy. X-rays are part of the electromagnetic spectrum; however, X-rays offer a sharper image because the wavelength of X-rays is shorter than the visible light wavelengths, as used in shadowgraphy. [9]. Another key difference between X-ray and optical methods is that optical methods tend to rely on the scattering of electromagnetic waves while X-ray methods tend to rely on absorption [9]. Because of this, X-ray scanning reflects the mass distribution of a substance or spray, and it gives X-ray techniques the ability to provide insight into the near-nozzle dense spray region [9, 10, 12-14].

X-rays have key characteristics that affect the measured properties and the manner of absorption. The photon energy of X-rays affects the amount of absorption and penetration. X-rays with high photon energy (12-120 keV or 0.10-0.01 nm wavelength) are considered hard X-rays, and they are absorbed less and penetrate more than X-rays with weaker photon energy. Weak X-rays are considered soft X-rays (0.12 keV-12 keV or 10-0.10 nm wavelength) [6, 9]. The absorption is also influenced significantly by the elemental composition of the substance

being measured. Because the amount of absorption generally relates to atomic numbers, different elements absorb different wavelengths of X-rays [9]. For example, all elements tend to absorb weaker X-rays primarily.

X-ray sources can be either monochromatic or polychromatic. Monochromatic X-rays involve a single X-ray wavelength while polychromatic involve a wide range of wavelengths. In the case of polychromatic X-ray sources, lower-energy X-rays are disproportionately absorbed, which causes beam hardening [9, 15]. Careful calibration can help mitigate the effects of beam hardening. Additionally, additives of heavy elements to the measured substance can provide more contrast by absorbing more hard X-rays.

X-ray CT can be implemented using one of several different types of X-ray sources to create projections. Two options that have been used for spray imaging are synchrotrons and laboratory sources. Synchrotrons are the more expensive of the two and provide more versatility to the user than laboratory X-ray sources. Synchrotrons employ high-energy particle beams that emit electromagnetic radiation. These beams are very narrow and emit in a forward cone [9]. Providing a high flux of photons improves resolution and signal-to-noise ratio, making synchrotron sources well-suited to spray analysis applications. In addition, a synchrotron can more easily be made quasi-monoenergetic than hospital grade sources, thereby mitigating the effects of beam hardening [9]. Synchrotron sources also have a key advantage in that they provide very short pulses of X-rays, which allows them to provide time-resolved reconstructions [16, 17]. Because of the narrow beam emitted, synchrotrons provide a small range of measurement and are not always suitable to measure larger objects. Another significant limitation of synchrotrons is their cost, which is often over $200 million [18].

The challenges of access, field-of-view, and high cost of synchrotron sources has motivated researchers to consider the use of hospital grade or laboratory system X-ray sources. Hospital grade systems offer a smaller and less costly alternative (approximately $50,000 USD) [19]. A laboratory X-ray source has much lower flux than produced by a synchrotron, and the focal spot size is larger, so exposure times are longer, and the resulting image resolution is lower.

NOZZLES

For both the shadowgraphy and X-ray experiments, the same two custom-made pressure-swirl atomizers were utilized. Due to the relatively low resolution of the X-ray CT system, both nozzles were large, but non-dimensional parameters describing the flow were matched to those typically measured when using smaller nozzles to ensure consistency. In fuel atomizers, the orifice diameter, d_0, is generally around 150 μm, but the nozzles in this experiment had diameters of 2 mm and 3 mm due to the relatively low resolution of the X-ray CT system. Both nozzles had a hollow-cone pressure swirl design. Within this nozzle design, liquid swirls around an air-cored vortex. Upon exiting, the fluid expands due to its radial velocities, forming a conical sheet which becomes unstable and breaks up into droplets. Such nozzles are commonly used in combustion applications due to their simplicity, high atomization, and wide spray cones [1].

Dimensionless Parameter	**2 mm Atomizer**	**3 mm Atomizer**
L_s/D_s	1	1
D_s/d_0	3	3
l_p/d_p	1.6	1.6
d_0/l_0	1	1
Dimensional Parameter	**2 mm Atomizer**	**3 mm Atomizer**
d_0 [mm]	2	3
l_0 [mm]	2	3
D_s [mm]	6	9
L_s [mm]	6	9
d_p [mm]	1.2	1.8
l_p [mm]	2	3
Θ [°]	45	45

Table 1: Dimensionless and dimensional parameters for each nozzle and experiment

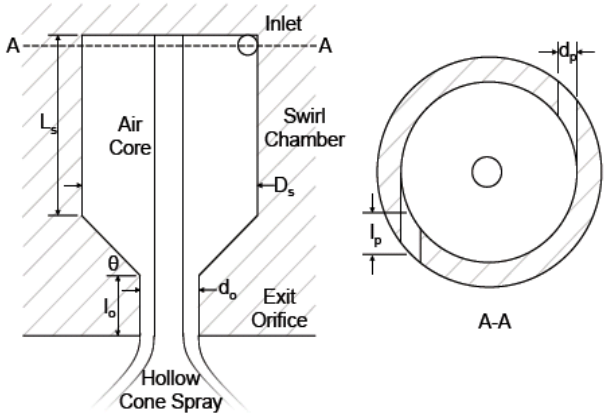

Figure 2: Typical geometry of a hollow cone atomizer [20]

To ensure consistency, the nozzles were designed with equal non-dimensional parameters. Table 1 lists the various dimensionless and dimensional parameters used, and Figure 2 illustrates these parameters [20]. Both nozzles

were manufactured using stereolithography, which yields high geometrical accuracy [20].

SHADOWGRAPHY EXPERIMENTS

The shadowgraphy experiments were conducted at the U.S. Army Research Laboratory's Spray and Combustion Research Laboratory in Aberdeen Proving Ground, MD. The setup involved spraying water through each nozzle into a transparent, cylindrical spray chamber as shown in Figure 3. The water flow was adjusted by modifying the pressure until the velocity reached the desired value for the Reynolds and Weber numbers. The nozzles used were the exact ones used during CT scanning. A Photron SA5 Fastcam camera recorded the spray at 40,000 frames per second using an exposure time of $1x10^{-6}$ seconds. A LED light source was located directly across the chamber from the camera and was positioned behind a diffuser to provide a consistent intensity of light across the camera. After spraying in front of the camera, the water flowed out of the system through tubing at the bottom of the test chamber. The camera was scaled and focused using a calibration plate with spacings of a known separation. Calibration was conducted prior to the spray experiments and each time the camera was moved to a different position. Flow rates were calculated by measuring the volumetric flow into a graduated cylinder after one minute. Using the calculated volumetric flow rate along with the known orifice size of each nozzle, a mean velocity was calculated. In combination with known values for surface tension, density, and

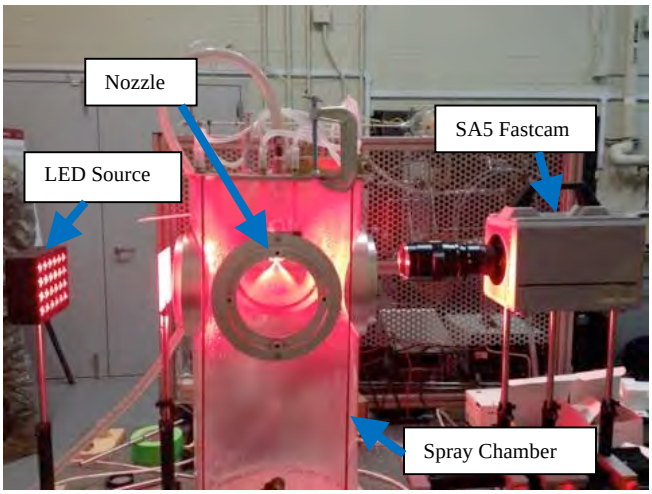

Figure 3: Shadowgraphy experimental setup

dynamic viscosity, values for Reynolds and Weber numbers were calculated. These values are presented in Table 2. The relative uncertainty for the Reynolds and Weber number is estimated to be 10% due to uncertainties in the spray velocity, surface tension, and viscosity.

For the shadowgraphy experiment, tap water was used, but a solution of distilled water with 20% Isovue-370 (by volume, to increase X-ray image contrast) was used for the X-ray CT experiment. This led to differences in the Weber and Reynolds numbers between the experiments, and their respective calculated values are displayed in Table 2.

		2 mm	3 mm
Re	**Shadowgraphy:**	37000	68000
	X-ray CT:	26000	40000
We	**Shadowgraphy:**	10000	22000
	X-ray CT:	11000	17000

Table 2: Reynolds and Weber numbers

X-RAY CT EXPERIMENTS

The X-ray CT Scanning experimental setup is described in detail elsewhere [20]. The setup employed an X-ray source across from an X-ray detector with the spray chamber between the two, as shown in Figure 4. The X-ray source was a medical-grade tube with a Varian G-1593bi insert and a B-180H housing. The detector was a Varian PaxScan 4030CB amorphous silicon digital detector. The X-ray source was located 1422 mm away from the rotation axis of the spray system, and the detector was 398 mm on the opposite side. Operating at a photon energy of approximately 40 kV and 50 mA permitted image acquisition of chamber and atomizer, while also providing sufficient absorption by the spray. The two-dimensional images had a resolution of 1024 by 768 pixels. The acquisition rate for all experiments was 15 frames per second. Additionally, 16 CT acquisitions for each nozzle were conducted to permit averaging and improved image statistics and to ensure reproducibility between results.

To allow for projections from 360º around the spray axis, the cylindrical spray chamber was rotated in 1250 equally spaced increments. The X-ray source and detector were mounted on a Newport RP Reliance optical bench and remained stationary during experimentation. A three-dimensional spray mass distribution was reconstructed from the 1250 images using computed tomography techniques.

Because X-ray image contrast depends heavily on the attenuation coefficient of the spray, a 20% volume fraction of Isovue 370 with 80% water was used. This solution has a kinematic viscosity of 1.26×10^{-6} m^2/s, but it increases the attenuation coefficient by a factor of 4 over that of pure water, which significantly improves the visibility of the spray. The Weber and Reynolds number for each nozzle in this experiment are shown in Table 2.

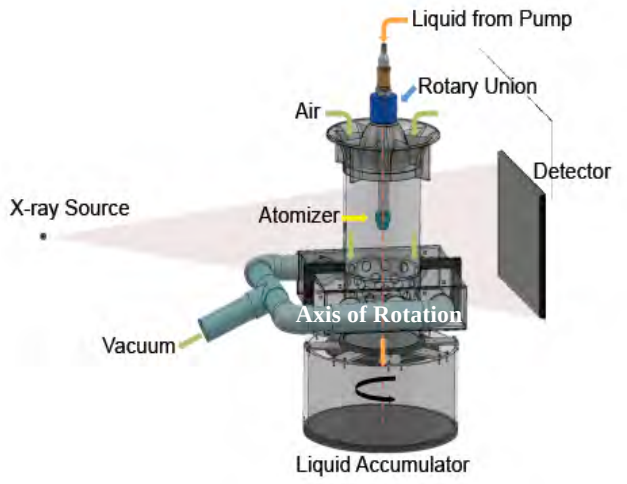

Figure 4: X-ray CT scanning experimental setup [20]

Besides the addition of the rotating platform, the cylindrical chamber in this experiment was similar to that of the shadowgraphy experiments. The low-density and small thickness of the chamber walls helped mitigate any beam hardening effects that would create artifacts [20]. To minimize droplet buildup on chamber walls, a co-flow system using a blower to draw air downwards was installed [9, 18]. As seen in Figure 5, droplet accumulation still occurred in the lower portions of the chamber, limiting the length of the measurement domain.

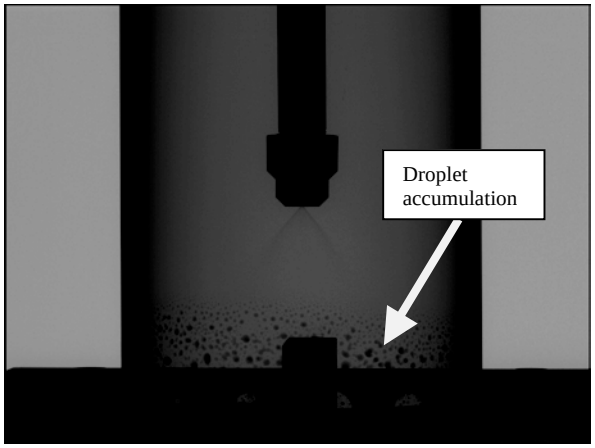

Figure 5: Droplet accumulation along the bottom of the X-ray CT test chamber [20]

SHADOWGRAPHY PROCESSING

LaVision's Data Acquisition and VISualization (DAVIS) Software (Version 8) was used to analyze the shadowgraphy images. The DAVIS Software allowed for analysis of the spray cones and droplets. As with all shadowgraphy methods, insight in the near-nozzle region was limited by the high degree of refraction and absorption of the light, which resulted in measured intensity values of zero.

In order to effectively compare images from shadowgraphy, the software was used to create a time-averaged image from 2500 frames of the spray from 5 different data sets, which corresponds to an averaging over 0.0625 seconds. Time-averaging gave an accurate image of the average spray cone angle and perimeter of the conical spray. By defining various parameters such as nozzle exit and light intensity values, spray cone angle and skew were determined. Time-averaged images were used to match the X-ray CT analysis and to avoid random variations in individual images due to spray unsteadiness.

Shadowgraphy images can be processed to determine droplet properties. This is a key advantage of shadowgraphy over CT scanning. To process the data, a filter to smooth out the variations in background light is defined. Then, an intensity value is set to define potential particles. All pixels with this intensity value or greater are considered to be potential particles. This definition is refined by setting a low and high intensity threshold within all potential particle pixels. All particles that fall above the first intensity level and within the refined one are counted and marked on each image. The software tracks particles to ensure it does not count the same particle twice between multiple frames. Lastly, a particle list of every recognized particle with corresponding statistics is produced [21]. This list was used to create a distribution plot for each set of conditions. Further details regarding droplet processing can be found in [22].

X-RAY CT PROCESSING

Each CT scan collected 1250 images while the chamber rotated 360º in order for a proper 3D reconstruction to be conducted. Prior to scanning, a gain calibration was conducted in order to zero the background on the detector. Using this image, the ViVA Rev K.05 Build 67 software sets the intensity value of each pixel to zero. This ensures that the intensity values are uniform when conducting the data analysis.

In X-ray computed tomography there are two determinants of image quality: noise and artifacts. Artifacts are irregularities on an image caused by improper calibration to items of interest. These are greatly reduced by the choice of material placed in the CT unit. Noise, however, is a random phenomena in radiology, and there are several processes that can cause it. These include the number of photons that leave the source, the number of photons that pass unaffected through the object, and the number of photons captured by the detector [23]. Steps were taken during set-up, experimentation and processing to help decrease the noise.

During data acquisition, the software was set up to conduct 2x2 binning to produce a projection image of 1024 by 768 pixels. 2x2 binning was conducted with 1250 images as opposed to 1x1 binning with 625 images. The binning allowed for the effects of minor observation errors to be reduced by taking a central value over a 2x2 interval

of pixels. Improved signal to noise ratio results from using the 2x2 binning at the expense of halved spatial resolution.

Once the image was taken, a region of interest was cropped out of the full image. The region of interest was defined as the top of the swirl chamber to approximately 30 nozzle diameters downstream. This was done to reduce processing time spent on areas without spray.

For this experiment, a cone beam reconstruction was conducted based upon the X-ray tube source. For the region of interest, the following parameters were used to conduct the reconstruction. The number of voxels in the x and y directions (plane parallel to ground) was 1024 and in the z direction (normal to ground plane) 256. The origin was defined as the center of the orifice of the nozzle. The dimension in the x/y direction was 332.8 mm and 83.2 mm in the z direction. From the 1250 frames, 256 CT slices along the z axis were reconstructed. MATLAB code was used to combine these slices together to create the 3D reconstructed images. The 16 CT scans were then averaged to produce a voxel size of 325 x 325 x 325 μm^3. The 16 sequential CT acquisitions helped ensure a high signal to noise ratio.

SHADOWGRAPHY RESULTS

Time-averaged images were analyzed for spray cone angle and skew. Skew defines the right cone angle minus the left. Figure 6 shows a near-instantaneous image next to time-averaged image over 62,500 µs with the spray cone angle definition overlaid for the 3 mm nozzle. With regard to spray cone angle and skew, the spray showed a high degree of consistency. Table 3 shows the results for each nozzle.

Table 3: Shadowgraphy spray cone data

	2 mm nozzle	**3 mm nozzle**
Spray Cone Angle [º]	74.9	79.2
Skew [º]	-1.3	-0.2

With shadowgraphy, the spray cone angle, skew, and particle sizes were measured. However, there are limitations to these measurements. Because shadowgraphy is inherently a two-dimensional projection of a three-dimensional spray, asymmetries in the spray cone may appear different depending on the orientation of the camera to the nozzle. While the nozzles are designed to be symmetrical, small errors in manufacturing or machining can create asymmetries [5]. Shadowgraphy can only measure asymmetries that exist in the plane perpendicular to the camera's line of sight. For this reason, shadowgraphy is limited in its analysis of spray cones. Furthermore, it cannot closely examine the near-nozzle region. Near the nozzle, the spray is sufficiently dense to reduce pixel intensity to zero. Therefore, the average spray density cannot be determined in this region.

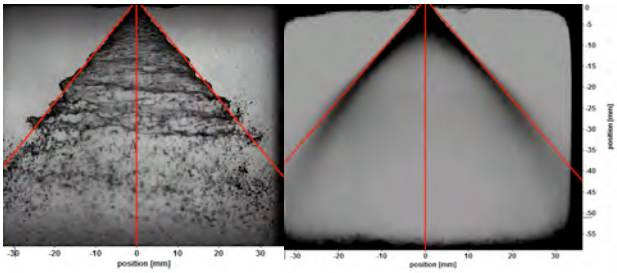

Figure 6: 25 µs (left), average over 62,500 µs (right) with 3 mm nozzle

Particle analysis was also conducted for each nozzle at both 138 kPa and 276 kPa in a 2 mm by 2mm area 25 nozzle diameters downstream of the nozzle exit. The results of this analysis are shown in Figure 7.

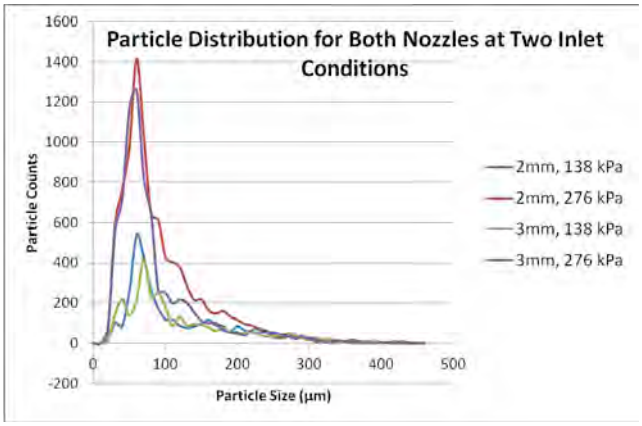

Figure 7: Shadowgraphy particle analysis for 2 mm and 3 atomizers at 138 kPa and 276 kPa

As expected, the droplet size distributions show that the majority of the particles are less than 100 microns, which is relatively small given the large nozzle sizes. The long tails indicate rare large droplets. As the pressure is increased, the number of droplets increases significantly and the peak shifts slightly to the smaller droplet size. Quantitative statistical data are presented in Table 4, which confirm the distributions from Figure 7. The Sauter mean diameter (D32) is the diameter of a representative drop that has a volume to surface area ratio of that of the entire spray. The mass median diameter (DV50) is a representative diameter of a drop for which the 50% of the total liquid volume of the spray is composed of smaller drops [1].

	2mm, 138 kPa	**2mm, 276 kPa**	**3mm, 138 kPa**	**3mm, 276 kPa**
N	3857	10161	3565	8165
D10 (µm)	122	93	127	87
D32 (µm)	233	192	256	207

DV50 (μm)	346	283	378	325

Table 4: Statistics on each of the nozzles under 138 kPa and 276 kPa where N is number of observed particles

X-RAY CT RESULTS

Time-averaged liquid concentration distribution, C, results are presented both inside the nozzles and for a distance of approximately ten orifice diameters downstream for both the 2 mm and 3 mm atomizers. Figure 8 shows a

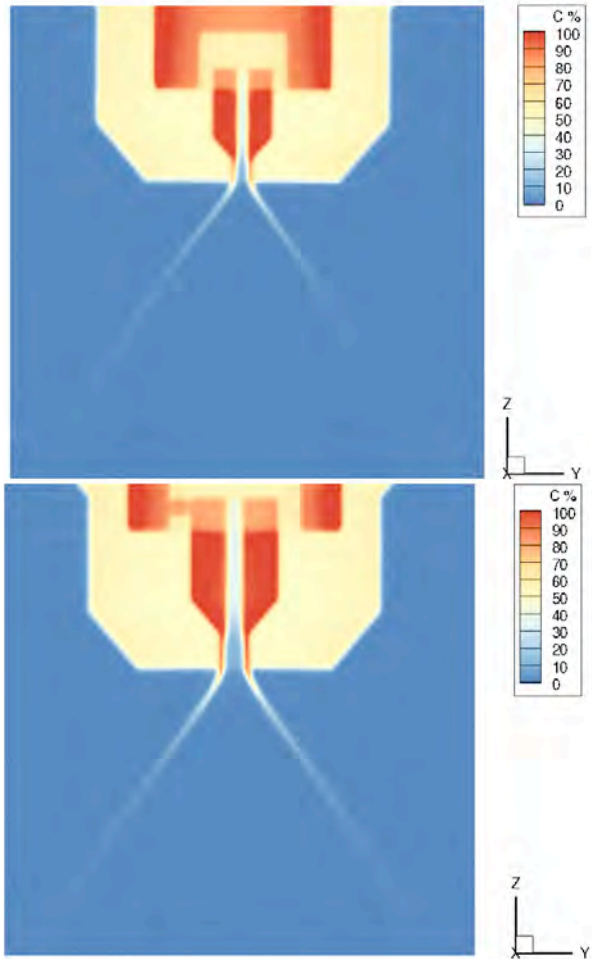

Figure 8: Cross-sectional slices of liquid concentration distribution along x=0 plane for the (top) 2 mm atomizer and (bottom) 3 mm atomizer

cross-sectional slice taken from the averaged 3D reconstruction of liquid concentration distribution along the x=0 plane for both nozzles. The origin of the coordinate system set at the center of the exit orifice with the z-axis oriented along the direction of the spray.

Both nozzles display spray characteristics typical of pressure swirl atomizers. A nominally axisymmetric hollow cone spray is formed immediately after the exit orifice with an air-cored vortex that extends to the top of the swirl chamber formed upstream of the exit orifice. The air-core vortex is difficult to examine using conventional optical techniques, but can be readily visualized using X-ray CT imaging. Since the air-core plays an important role in the development of the spray, improvements to the X-ray technique will yield key insight into fluid behavior within the nozzle itself.

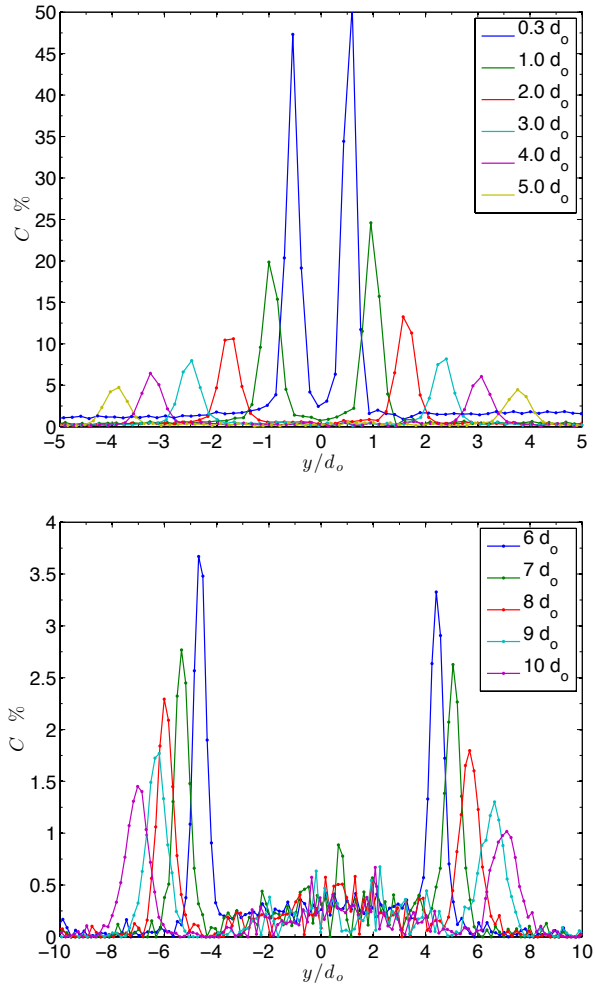

Figure 9: Spray profiles of liquid concentration distribution at different downstream distances along the x=0 plane for the 2 mm atomizer

Spray profiles of liquid concentration along the x=0 plane at different distances downstream of the exit orifice for the 2 mm and 3 mm atomizers are shown in Figure 9 and Figure 10, respectively. The spray profiles demonstrate that there is slight variation in the liquid concentration with azimuthal angle. The non-zero concentration within the hollow cone downstream is most likely the contribution of liquid droplets within the hollow cone spray. This behavior has been shown in other experiments [10].

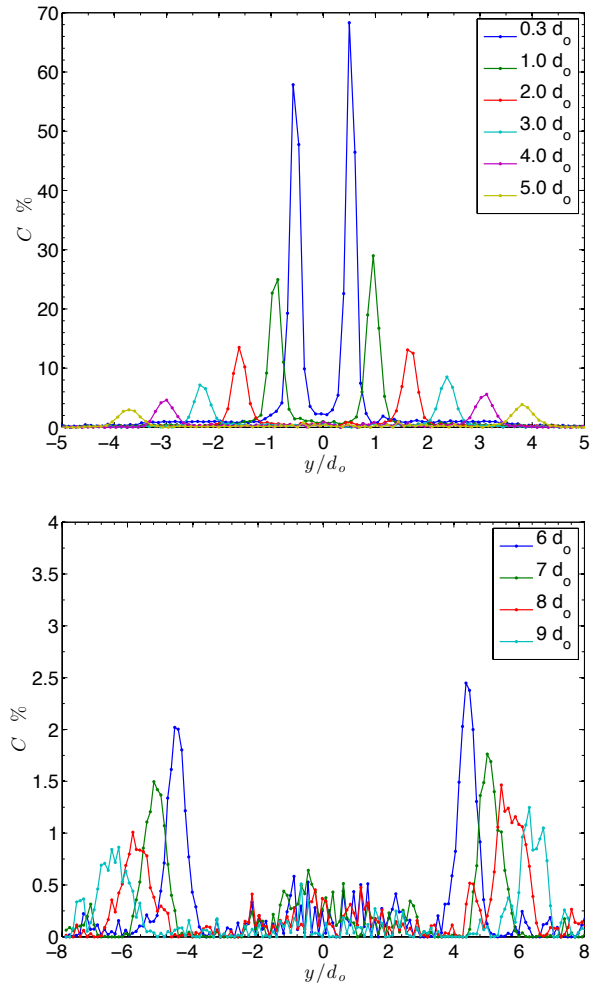

Figure 10: Spray profiles of liquid concentration distribution at different downstream distances along the x=0 plane for the 3 mm atomizer

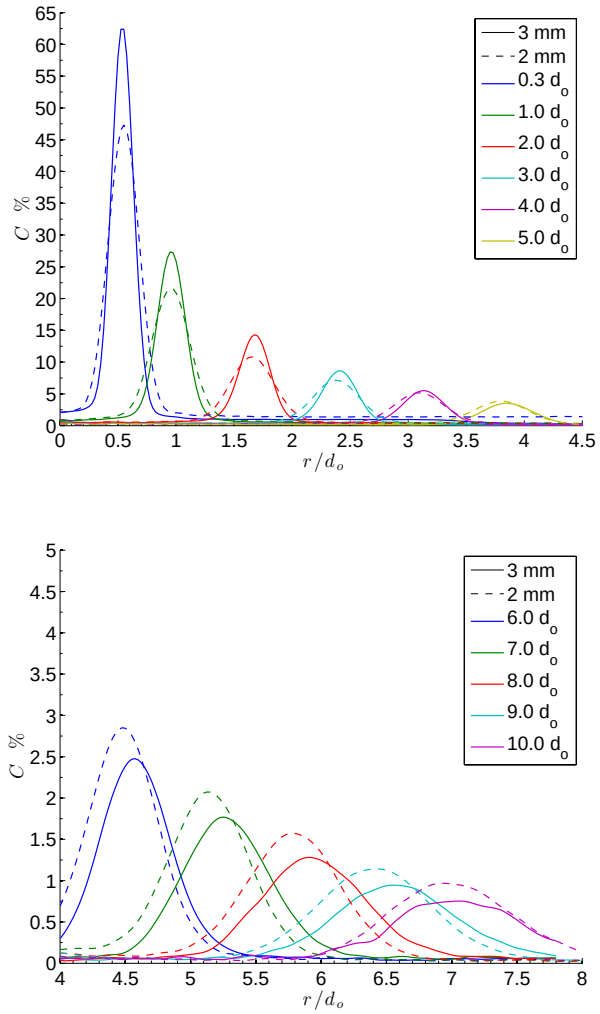

Figure 11: Averaged radial spray profiles of liquid concentration at different downstream distances for the 2mm and 3mm atomizer

Figure 11 shows the azimuthally averaged spray profile of liquid concentration at different downstream distances for both the 2 mm and 3 mm atomizer. The liquid concentration is already below 100% immediately after the exit orifice and drops rapidly to below 5% by five orifice diameters downstream for both atomizers. Although the liquid sheet has not yet broken up into droplets, the unsteady motion of the sheet reduces the time-average density at any given point. Based on the peak location of liquid concentration from the radial spray profiles up to 5 nozzle diameters downstream, the spray angle for the 2mm and 3mm atomizer is approximately 69° and 71°, respectively.

Figure 12 shows iso-surfaces of 3% liquid concentration along with a cross-sectional slice along the x=0 plane with a 3% liquid concentration cutoff level for ease of visualization for both the 2mm and 3mm atomizer, which demonstrates the three-dimensional nature of X-ray CT imaging. Using iso-surfaces of varying concentration, complex three-dimensional structures can be readily visualized.

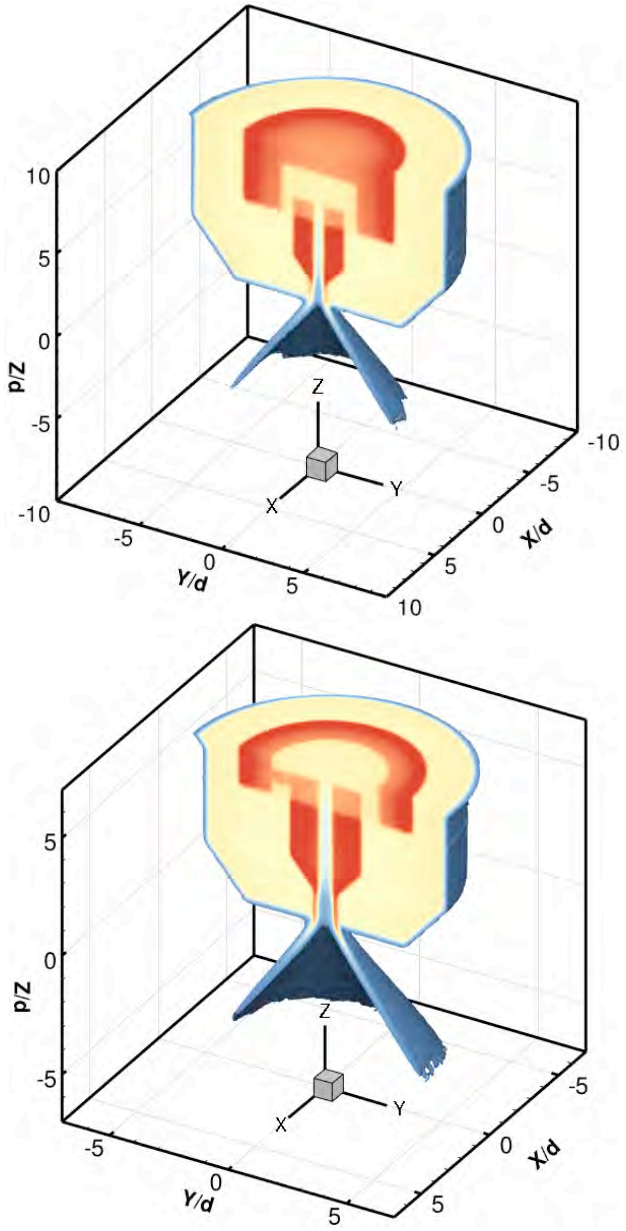

Figure 12: Iso-surface of 3% liquid concentration and slice along $x = 0$ plane with a 3% liquid concentration cutoff level for both the (top) 2mm atomizer and (bottom) 3mm atomizer

COMPARISON OF RESULTS

While shadowgraphy and X-ray CT scanning have different abilities, there is still overlap in their yielded insights. The shadowgraphy technique used in this study has a key advantage in that it can provide near-instantaneous images. It can provide droplet analysis and show the time-resolved structure of a spray in portions where light is refracted. X-ray CT scanning provides unique insight into the mass distribution of the spray, and it can also provide analysis inside of and immediately outside of the nozzle.

While the experiments were similar in approach, there exist important differences in them. The most significant of these is that X-ray CT scanning illustrates mass distributions while shadowgraphy only shows variations in scattered light. In this case, the X-ray CT system also allowed for imaging from all sides while the shadowgraphy did not.

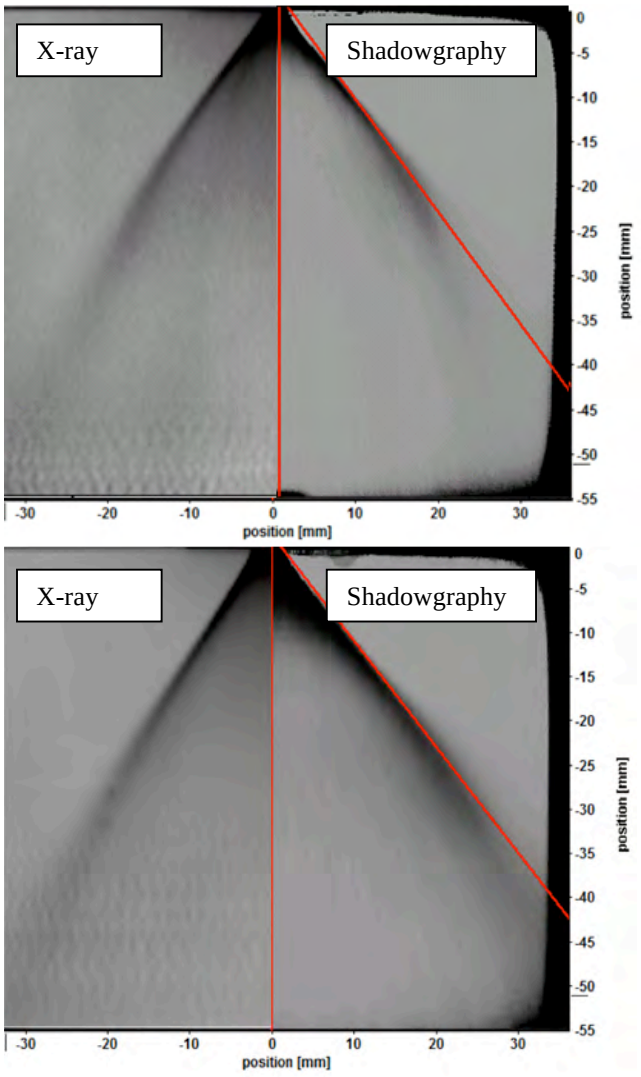

Figure 13: Technique comparisons for the 2mm nozzle (top) and 3mm nozzle (bottom)

The two methods, while using different approaches, both can give information on the near-nozzle region. The CT results show much more quantitative details, as shown in the three-dimensional tomographic reconstructions. Shadowgraphy can provide details on the spray structure right after exiting the nozzle, but it does not show mass distribution (only differences in light intensity). In this

capacity, X-ray CT scanning provides more detail of spray symmetry and changes in liquid distribution in various locations away from the nozzle. Shadowgraphy can provide spray cone angles and skew, and it has been shown the ability to produce 3D reconstructions with multiple cameras [11]. In principle, a tomographic reconstruction of shadowgraphy data could also be done if a rotation system was used to acquire images from many angles. However, this capability has not been demonstrated, and it is unlikely that a standard X-ray CT algorithm could be used to provide quantitative 3D data from shadowgraphy images.

In analyzing the spray dispersion, the two methods result in slightly different spray cone angles. For example, the three-millimeter nozzle results in a 79.2º spray cone angle using shadowgraphy but a 71º using X-ray CT analysis. This discrepancy can likely be attributed to the intensity values that each method detects or the threshold values used for analysis. Shadowgraphy defines the spray according to light intensities, while X-ray CT scanning uses X-ray absorption. Due to these differences, shadowgraphy is better able to capture the full extent of fluctuations in spray. Figure 13 shows a side-by-side comparison of the X-ray CT spray structure with that of the shadowgraphy.

Overall, by approaching spray analysis from different methods, shadowgraphy combined with X-ray CT scanning can provide a practical and holistic approach to spray analysis. Alone, each method has several limitations, but when used together, each method covers many of the other's limitations. Shadowgraphy can provide particle analysis, but it also complements X-ray CT scanning through visualization of the breakup region and measurement of a full spray cone angle. Likewise, X-ray CT scanning complements shadowgraphy by providing three-dimensional spray analysis, mass distribution, and insight into the dense spray regions.

CONCLUSIONS

The objective of this work was to demonstrate the capabilities and complementary aspects of shadowgraphy and X-ray CT scanning. Experimentation on the same nozzles illustrates the effects of analyzing sprays using both techniques. Neither method alone provides complete insight of a spray.

Future work includes implementing a rotating nozzle in the shadowgraphy experiment to compare three-dimensional results from each method. Additionally, better calibration of instruments and improved X-ray resolution will also be subjects of future work. To better illustrate the accuracy of each method, analysis will be conducted on a similar nozzle with an asymmetric orifice.

ACKNOWLEDGMENTS

This work was funded, in part, by the Army Research Office (Cooperative Agreement #W911NF-13-2-0048). The authors would like to acknowledge Dr. Waldo Hinshaw for his work on the X-ray CT experiments at Stanford University.

NOMENCLATURE

$d_{0:}$ Orifice Diameter
d_p: Inlet Diameter
D_s: Swirl Chamber Diameter
l_0: Orifice Exit Length
l_p: Inlet Length
L_s: Swirl Chamber Length
N: Number of Particles
D10: Mean Diameter
D32: Sauter Mean Diameter
DV50: Mass Median Diameter
Re: Reynolds Number
We: Weber Number

REFERENCES

[1] Lefebvre, A. H., 1989, *Atomization and Sprays*. Hemisphere Publishing Co., New York.

[2] Coghe, A. and Cossali G. E., 2012, "Quantitative optical techniques for dense sprays investigation: A survey," *Optics and Lasers in Engineering*, Vol. 50, pp. 46-56.

[3] Gharsallaoui, A., Roudaut, G., Chambin, O., Voilley, A., Saurel, R., 2007, "Applications of spray-drying in microencapsulation of food ingredients: An overview," *Food Research International*, Vol. 40, pp. 1107-1121.

[4] Bailey, A. G.,, 1988, *Electrostatic Spraying of Liquids* Research Studies Press Ltd., Somerset, England.

[5] Liu, X., Im, K., Wang, Y., Wang, J., Tate, M., Alper, E., Schuette, D., Gruner, S., 2009, "Four dimensional visualization of highly transient fuel sprays by microsecond quantitative x-ray tomography," *Applied Physics Letters*, Vol. 94.

[6] Linne, M., 2013, "Imaging in the Optically Dense Regions of a Spray: A Review of Developing Techniques," *Progress in Energy and Combustion Science*, Vol. 39, pp. 403-440.

[7] Wang, Q., 2012, *Advanced Optical and 3D Reconstruction Diagnostics for Combustion and Fluids Research*. University of Sheffield.

[8] Settles, G. S., 2001, *Schlieren and Shadowgraph Techniques*. Springer-Verlag, Inc. Berlin.

[9] Kastengren, A., Powell, C., 2014, *Synchrotron X-ray techniques for fluid dynamics.* Springer-Verlag, Inc. Berlin.

[10] Lim, J., Sivathanu, Y., Wolverton, M., 2013, "Evaluation of Soft X-Ray Absorption Tomography for the Near Injector Characterization of Dense Sprays," *ILASS Americas, 25th Annual Conference on Liquid Atomization and Spray Systems*.

[11] Wang, Q. and Zhang, Y., 2011, "High Speed Stereoscopic Shadowgraph Imaging and its Digital 3D Reconstruction," Measurement Science and Technology, Vol. 22, No. 6, pp 1-9.

[12] Balewski, B., Heine, B., Tropea, C., 2008, "Experimental Investigation of the Correlation Between Nozzle Flow and Spray using LDV, PDA, High-speed Photography and X-Ray Radiography," *ILASS Europe, 22nd Annual Conference on Liquid Atomization and Spray Systems*.

[13] MacPhee, A. G., Tate, M. W., Powell, C. F., Yue, Y., Renzi, M., Ercan, A., Narayanan, S., Fontes, E., Walther, J., Schaller, J., Gruner, S., Wang, J., 2002 "X-ray Imaging of Shock Waves Generated by High-Pressure Fuel Sprays," *Science* Vol. 295 pp. 1261-1263.

[14] Meyer, T. R., Schmidt, J., B., Nelson, S. M., Drake, J., Janvrin, D., Heindel, T., 2008, "Three-Dimensional Spray Visualization using X-ray Computed Tomography," *ILASS Americas, 21st Annual Conference on Liquid Atomization and Spray Systems*.

[15] Yan, C. H., Whalen, R. T., Beaupré, G. S., Yen, S. Y., Napel, S., 2000, "Reconstruction Algorithm for Polychromatic CT Imaging: Application to Beam Hardening Correction," *IEEE Transactions on Medical Imaging*, Vol. 19, No. 1.

[16] Powell, C. F.,, Yue, Y., Poolab, R., Wang, J., 2000, "Time-resolved measurements of supersonic fuel sprays using synchrotron X-rays," *Journal of Synchrotron Radiation*, Vol. 7, pp. 356-360.

[17] Wenyi, C., Powell, C., Yue, Y., Narayanan, S., Wang, J., Tate, M., Renzi, M., Ercan, A., Fontes, E., Gruner, S., 2003, "Quantitative analysis of highly transient fuel sprays by time-resolved x-radiography," *Applied Physics Letters*, Vol. 83, No. 8, pp. 1671-1673.

[18] Centre for Learning Technology, The University of Western Australia, 2013, "Synchrotron Investigations," Australia School Innovation in Science, Technology, & Mathematics.

[19] Siemens ISO-C Mobile C-Arms. MedScan Diagnostic Systems, Inc. 2014 http://c-armequipment.com/special-offers.html

[20] Guzman, P. A., Eaton, J., Fahrig, R., Coletti, F., and Benson, M., 2014, "Near-Field Spray Measurements Using X-ray Computed Tomography," *ILASS Americas, 26th Annual Conference on Liquid Atomization and Spray Systems*.

[21] LaVision Data Acquisition and Visualization Software 8, 2012, "Product Manual: ParticleMaster Shadow," Gottingen, Germany.

[22] Ryan, M., Tennis, J., Eichner, D., Lee, Z., Sowell, T., Benson, M., Van Poppel, B., Kurman, M., Kweon, C-B., 2014, "Experimental Results of an Electrostatic Injector," *ILASS Americas, 26th Annual Conference on Liquid Atomization and Spray Systems*.

[23] Eichner, D., 2013, "Utilizing X-ray Computed Tomography in Spray Nozzle Analysis," IMECE2013-65329

